Research Square

Preprints are preliminary reports that have not undergone peer review.
They should not be considered conclusive, used to inform clinical practice,
or referenced by the media as validated information.

Concentration-Dependent Membrane Interactions and Pore Stability of Aurein 1.2 and LLAA Revealed by Coarse-Grained Molecular Dynamics Simulations

Roshanak Ansarihaghi

roshanak.ansari@ut.ac.ir

Institute for Advanced Studies in Basic Sciences

Research Article

Keywords: antimicrobial peptides, aurein 1.2, LLAA, molecular dynamics simulation, coarse-grained simulation, membrane interactions

Posted Date: July 7th, 2026

DOI: https://doi.org/10.21203/rs.3.rs-10181139/v1

License: This work is licensed under a Creative Commons Attribution 4.0 International License.
Read Full License

Additional Declarations: No competing interests reported.

Concentration-Dependent Membrane Interactions and Pore Stability of Aurein 1.2 and LLAA Revealed by Coarse-Grained Molecular Dynamics Simulations

Roshanak Ansarihaghi[1,2*]

[1]Department of Biological Sciences, Department of Biophysics, Institute for Advanced Studies in Basic Sciences, Zanjan, 45137-66731, Iran.
[2]Department of Biophysics, Institute of Biochemistry and Biophysics, University of Tehran, , Tehran, 1417614411 , Iran.

Corresponding author(s). E-mail(s): roshanak.ansari@ut.ac.ir;

Abstract

Aurein 1.2 is a short cationic antimicrobial peptide secreted by the Australian tree frog *Litoria aurea*. In this study, we investigated the interaction of aurein 1.2 and its analogue (LLAA) with membrane models of different compositions using coarse-grained molecular dynamics simulations with the MARTINI force field. Our results show that LLAA exhibits stronger interactions with lipid bilayers compared with aurein. Both peptides demonstrated a greater tendency toward bacterial membranes (POPE/POPG) relative to eukaryotic membranes (POPC and DPPC). LLAA also displayed a higher propensity to separate from the initial peptide population, facilitating deeper membrane insertion. This observation indicated that membrane penetration is enhanced when peptides adopt a single, separated state. Analysis of pre-formed pore simulations revealed distinct behaviors for the two peptides. In LLAA systems, only one of five peptides remained vertically inserted, while the remaining peptides relocated toward the membrane surface and adopted horizontal orientations. In contrast, aurein pores remained structurally stable throughout the simulations. Furthermore, pores in POPE/POPG bilayers exhibited greater stability than those in DPPC membranes. Altogether, these findings demonstrate how subtle differences in peptide sequence and charge distribution govern membrane interactions, insertion behavior, and pore stability.

Keywords: antimicrobial peptides, aurein 1.2, LLAA, molecular dynamics simulation, coarse-grained simulation, membrane interactions

1 Introduction

Antimicrobial peptides (AMPs) constitute a broad class of molecules synthesized by the innate immune systems of nearly all organisms to defend against pathogenic threats. These peptides are typically cationic, amphipathic, and relatively small, generally containing fewer than 50 amino acid residues. AMPs exert their biological activity at low micromolar concentrations and are primarily known for their membrane-targeting properties[1–3].

Beyond their essential role in host defense, AMPs have attracted considerable attention as potential next-generation antibiotics. Unlike conventional antibiotics, AMPs often exhibit reduced susceptibility to bacterial resistance mechanisms. Their selective activity is largely attributed to electrostatic interactions with membrane lipids, as bacterial membranes are enriched with negatively charged phospholipids, whereas eukaryotic membranes are predominantly neutral[4, 25].

AMPs operate through a variety of mechanisms. While some peptides disrupt membrane integrity, others interfere with intracellular processes such as cell division or cell-wall biosynthesis. Regardless of the specific pathway, membrane interaction represents a critical initial step. Several models have been proposed to describe AMP-induced membrane perturbation, including pore formation, surfactant-like membrane disruption, and translocation without stable pore formation[4, 26, 27].

Among the proposed mechanisms, the toroidal pore, barrel-stave, and carpet models are the most widely discussed. Although correlations between peptide length and mechanism remain debated, peptides longer than approximately 20 residues are often capable of spanning lipid bilayers in an α-helical conformation, facilitating pore formation. In contrast, shorter peptides are more frequently associated with surface-bound disruption mechanisms such as the carpet model[5]. In the carpet mechanism, peptides accumulate on the membrane surface until a threshold concentration is reached, triggering membrane destabilization. The toroidal pore model involves peptides stabilizing curved lipid headgroups within transmembrane pores, whereas the barrel-stave model describes peptide aggregates forming pore-like structures without substantial lipid bending[5, 6].

In the present study, we focus on aurein 1.2 and its analogue LLAA. Aureins comprise a family of AMPs secreted by the granular dorsal glands of Australian tree frogs, including *Litoria aurea* and *Litoria raniformis*[7]. Aurein 1.2 is a short cationic peptide containing 13 amino acids (GLFDIIKKIAESF-NH_2) and represents one of the smallest AMPs identified in vertebrates[5, 8]. This peptide adopts an amphipathic α-helical structure in membrane-mimetic environments but lacks a defined secondary structure in aqueous solution[6, 9]. Despite extensive experimental and computational investigations, its precise mechanism of membrane interaction remains under discussion. Previous studies have suggested carpet-like membrane disruption, while others

have reported membrane perturbation without stable pore formation[10–12]. Recent experimental work has further clarified the adsorption and insertion behavior of aurein 1.2 in charged lipid bilayers[25].

LLAA, the second peptide examined in this work, is a synthetic AMP derived from the human cathelicidin LL-37. Designed to probe sequence-dependent membrane interactions, LLAA contains 13 amino acids (RLFDKIRQVIRKF) and possesses a net charge of +5e, exceeding that of aurein 1.2. Owing to its increased cationicity, LLAA is expected to exhibit enhanced electrostatic interactions with negatively charged membranes. Structural studies have indicated that LLAA adopts conformations comparable to aurein 1.2 in both aqueous and membrane-associated environments[8].

Molecular dynamics (MD) simulations provide a powerful framework for investigating peptide-membrane interactions at atomistic and mesoscopic scales. Previous computational studies have demonstrated that peptide concentration, aggregation behavior, and electrostatic interactions critically influence membrane insertion and disruption mechanisms[26, 27]. These studies support the rationale for using MD simulations to investigate the single versus multi-peptide effects on membrane interactions.

2 Methods

Simulation Protocol and Force Field

Molecular dynamics (MD) simulations were performed using the GROMACS software package[13]. The MARTINI force field was employed for coarse-grained representations of the peptides in combination with the polarizable water (PW) model to improve the accuracy of electrostatic interactions. The three-dimensional structures of aurein 1.2 and LLAA were obtained from the Protein Data Bank (PDB), with codes 1VM5[14] and 2F3A[15], respectively. Both peptides are naturally amidated at their C-terminus. Accordingly, in the coarse-grained models, the backbone bead of the C-terminal residue was modified from Qa to Nda to reflect the neutralized terminus. To ensure charge neutrality, an appropriate number of Na^+ and Cl^- counterions were added. In two of the pore simulations, additional NaCl was included at a concentration of 0.15 M to mimic physiological ionic strength.

All simulations were conducted for 1 μs using a time step of 20 fs with the standard GROMACS molecular dynamics integrator, and the neighbor list was updated every 10 steps. Systems were equilibrated under NPT conditions for approximately 10 ns at 323 K using the V-rescale thermostat[16] with a coupling time constant of 1 ps. Pressure coupling was applied semi-isotropically using the Berendsen barostat[17], with a reference pressure of 1 bar, a time constant of 12 ps, and a compressibility of 3×10^{-4} (kJ mol^{-1} nm^{-3}). Electrostatic interactions were computed using the particle mesh Ewald (PME) method with a relative dielectric constant of 2.5 and a cutoff distance of 1.4 nm. Van der Waals interactions were treated using a shift function with a switch distance of 0.9 nm and a cutoff of 1.2 nm.

Peptide insertion into the bilayer and system solvation were performed using the `insane.py` script. Molecular visualization was carried out using VMD[18]. Quantitative analyses, including water counting within the bilayer, were conducted using

custom Tcl scripts executed in VMD. Average distances were calculated using a custom C++ program. Plots were generated using Grace software.

System Set-up

Coarse-grained molecular dynamics simulations were performed to investigate the interactions of aurein 1.2 and LLAA with lipid bilayers of varying compositions. All simulated systems were constructed within a $10 \times 10 \times 10$ nm^3 simulation box containing a lipid bilayer and one or more peptides. The detailed composition of each system, including the number of lipids per leaflet, water beads, and ions, is provided in Supplementary Table S**??**.

A total of 24 systems were simulated to examine concentration-dependent effects, comprising 12 single-peptide systems and 12 five-peptide systems. In these systems, peptides were initially positioned vertically adjacent to the membrane surface. The comparison between single- and multi-peptide configurations was designed to evaluate the influence of peptide concentration and collective behavior.

The lipid bilayer was oriented in the xy plane, while peptides were initially aligned along the z axis. To assess the impact of initial peptide orientation on membrane insertion, peptides were placed near the membrane surface in two distinct configurations: with either the C-terminal or the N-terminal region facing the bilayer.

To investigate peptide selectivity toward bacterial and eukaryotic membranes, simulations were conducted using model membranes of different compositions. Pure POPC and pure DPPC bilayers were selected to represent eukaryotic membranes, whereas POPE:POPG (3:1) bilayers were employed as bacterial membrane models. To further examine the effect of membrane charge density, simulations were repeated with a POPE:POPG ratio of 5:1. A summary of the simulated systems is presented in Table1.

Peptide insertion and peptide-lipid electrostatic interactions were used as indicators of membrane affinity. To quantify insertion behavior, distances between the membrane and key peptide residues – specifically, the C-terminal residue (Phe) and the N-terminal residue (Gly/Arg) – were calculated using the GROMACS tool `gmx distance`.

To explore additional concentration effects and alternative peptide arrangements, eight systems containing 1, 5, 10, and 20 horizontally oriented peptides were simulated for both aurein 1.2 and LLAA in the POPE:POPG (3:1) bilayer. In these systems, peptides were initially positioned at the membrane interface, with polar residues oriented toward lipid head groups and hydrophobic residues toward lipid tails.

Finally, pore stability was investigated using eight simulations in DPPC and POPE:POPG membranes. Pre-formed pores composed of five peptides were initially embedded at the membrane center. Each system was simulated for 1 μs to evaluate peptide rearrangement and pore stability. Representative snapshots of the initial pore structures and their structural evolution are shown in Fig. 4.

3 Results and Discussion

Single Vertical Peptides

MD simulations were performed to investigate peptide interactions with DPPC, POPC, POPE/POPG (3:1), and POPE/POPG (5:1) phospholipid bilayers. In this section, we present results for systems containing a single aurein or LLAA peptide initially positioned above the membrane. Because peptide absorption from bulk water into the membrane is a relatively slow process, peptides were initially placed vertically such that their terminal residues were in contact with the membrane surface. Each system was simulated for 1 μs.

As an example, the initial configuration and final state of the 1LLAA-N-POPE/POPG (3:1) system are shown in Fig. 1. The snapshots illustrate that the peptide, initially oriented vertically with its N-terminal facing the membrane (time = 0 ns), rapidly approached the bilayer and attached via its N-terminal residues (red beads) (time = 23 ns). Subsequent insertion occurred from the C-terminal region (green beads). By the end of the simulation (1 μs), the peptide exhibited slightly deeper insertion relative to earlier snapshots.

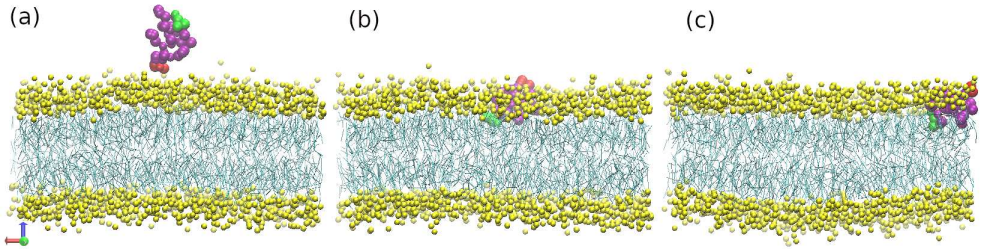


Fig. 1 Snapshots of the LLAA-N-POPE/POPG (3:1) system. (a) Initial configuration with LLAA positioned vertically above the membrane with the N-terminal facing the bilayer. (b) After 23 ns: peptide attachment via the N-terminal region (red beads). (c) At 1 μs: peptide insertion via the C-terminal region (green beads). Lipid head groups are shown in yellow and tails in cyan. Water molecules are omitted for clarity.

To quantify peptide insertion, distances between the membrane center of mass (COM) and key peptide residues – specifically, the C-terminal residue (Phe) and the N-terminal residue (Gly/Arg) – were calculated using the GROMACS tool `gmx distance`. Additionally, distances between lipid head groups and the membrane COM were computed to assess peptide penetration relative to the bilayer interface. These distance profiles are presented in Fig. 2.

The plots reveal that after only a few nanoseconds, the distance corresponding to the peptide C-terminal region decreases below that of the lipid head groups, indicating insertion from the C-terminal side. Across all systems, regardless of initial peptide orientation, peptides consistently attached via their N-terminal regions followed by C-terminal insertion. This behavior is supported by the representative snapshots shown in Fig. 1. Similar orientation behavior has been reported previously[20].

Peptide insertion was quantified based on the distance between the peptide C-terminal residue and the membrane COM. For comparison, the average distance between lipid head groups and the membrane COM was also calculated. Values averaged over the final 500 ns are reported in Table 1. The results confirm that initial peptide orientation does not significantly influence the final insertion depth.

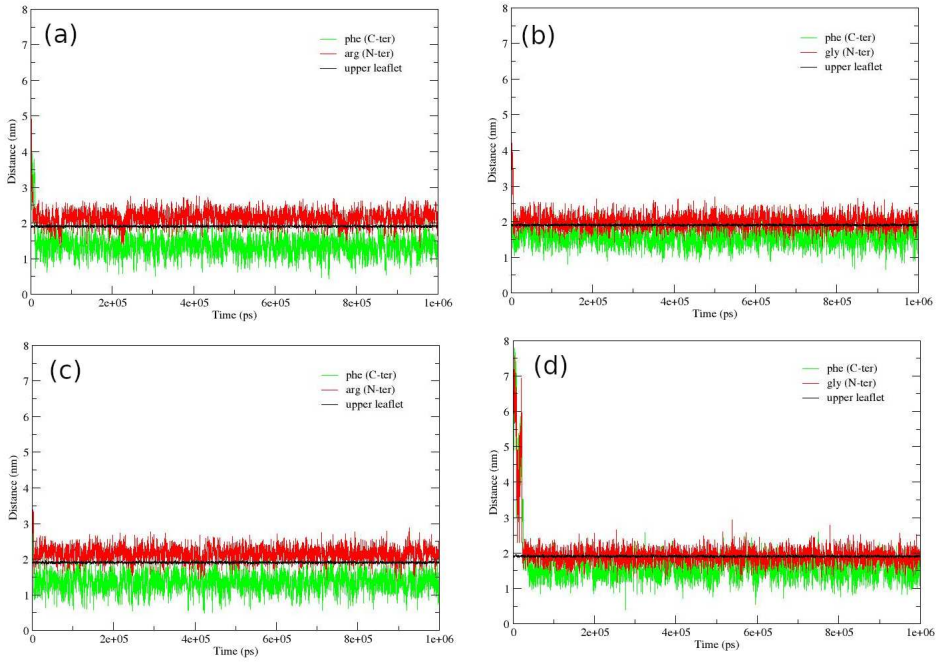


Fig. 2 Insertion dynamics of LLAA and aurein in POPE/POPG (3:1) bilayers. Distances between peptide terminal residues and the membrane COM over 1 μs simulations. Panels (a) and (b) correspond to initial C-terminal orientations, while (c) and (d) correspond to initial N-terminal orientations.

Consistent with Fig. 2, LLAA exhibits greater insertion relative to aurein across all membrane compositions. This trend is also reflected in Table 1. Given the higher cationic charge of LLAA, the enhanced insertion can be attributed primarily to stronger electrostatic interactions. Electrostatic interaction energies between peptides and lipids were evaluated using `gmx energy`, with averages calculated over the final 300 ns. As shown in Table S**??**, LLAA displays stronger electrostatic interactions with all membranes compared with aurein.
Furthermore, electrostatic interactions were stronger in bacterial membrane models relative to eukaryotic membranes, consistent with the negatively charged nature of bacterial bilayers. Correspondingly, both peptides demonstrated greater insertion into bacterial membranes (Table 1).

Table 1 Information about the systems simulated in this research. The peptide insertion (nm) is shown by calculating the distance between lipid head groups and C-terminal residue. Stability time of pores (ns) in systems with 5 peptides in pre-formed pores inside DPPC and POPE/POPG is considered based on continuous water permeation in the bilayer. Stars relevant to unexpected results

Single-peptide system	Insertion	Five-peptide system	Insertion	Pore system	Stability time
1aur-C-PEPG(3:1)	0.34	5aur-C-PEPG(3:1)*	0.20	Pore-5aur-DPPC	700
1aur-N-PEPG(3:1)	0.36	5aur-N-PEPG(3:1)	0.27	Pore-5LLAA-DPPC	$\sim$ 100
1LLAA-C-PEPG(3:1)	0.57	5LLAA-C-PEPG(3:1)	0.53	Pore-5aur-salt-DPPC	975
1LLAA-N-PEPG(3:1)	0.54	5LLAA-N-PEPG(3:1)	0.51	Pore-5LLAA-salt-DPPC	$\sim$ 30
1aur-C-PEPG(5:1)	0.33	5aur-C-PEPG(5:1) *	0.01	Pore-5aur-PEPG (3:1)	1500
1aur-N-PEPG(5:1)	0.37	5aur-N-PEPG(5:1)	0.50	Pore-5LLAA-PEPG (3:1)	$<$ 100
1LLAA-C-PEPG(5:1)	0.57	5LLAA-C-PEPG(5:1)	0.52	Pore-5aur-salt-PEPG (3:1)	1300
1LLAA-N-PEPG(5:1)	0.53	5LLAA-N-PEPG(5:1)	0.53	Pore-5LLAA-salt-PEPG(3:1)	$<$100
1aur-C-POPC	0.35	5aur-C-POPC	0.19		
1aur-N-POPC	0.35	5aur-N-POPC	0.38		
1LLAA-C-POPC	0.58	5LLAA-C-POPC	0.50		
1LLAA-N-POPC	0.51	5LLAA-N-POPC	0.50		

The insertion differences between LLAA and aurein were more pronounced in bacterial membranes than in eukaryotic bilayers. This observation suggests that while the peptides differ substantially in antibacterial potency, their hemolytic properties may differ only modestly.

No significant differences were observed between POPE/POPG ratios (3:1 vs 5:1), either in insertion depth or electrostatic interactions. Residue-level insertion analysis (Table S**??**) revealed insertion trends in the order:

POPE/POPG (3:1) ¿ POPE/POPG (5:1) ¿ POPC.

As shown in Fig. 2, the N-terminal region of LLAA remains primarily at the membrane surface, whereas the N-terminal region of aurein exhibits slight insertion into the bilayer. This difference can be attributed to residue composition. In LLAA, the N-terminal arginine, a positively charged residue, forms strong electrostatic interactions with negatively charged lipid phosphates, stabilizing its position near the membrane interface. In contrast, aurein contains glycine at the N-terminal position, which, due to its small size and weak polarity, is less restricted by electrostatic interactions and therefore displays limited penetration into the hydrophobic region.

Beyond the observed differences in terminal insertion, residue-level analysis provides further insight into peptide behavior. Calculation of the average distances of all amino acids from the membrane (Table S**??**) indicates that, in both peptides, hydrophobic residues preferentially insert into the bilayer core, while polar and charged residues remain closer to the membrane surface. Notably, hydrophobic residues in LLAA generally exhibit deeper insertion relative to those in aurein. In aurein, charged and polar residues remain largely surface-associated, whereas in LLAA, several charged residues (Lys and Arg) display partial insertion into the membrane (data not shown). A more detailed examination of LLAA insertion reveals that small hydrophobic residues adjacent to polar or charged residues exhibit reduced insertion depths compared with

hydrophobic residues located farther from charged sites. This behavior is consistent with electrostatic constraints imposed by neighboring hydrophilic residues interacting with lipid head groups. Effectively, hydrophobic residues experience positional restrictions due to their proximity to charged residues. However, Ile6 and Ile10 in LLAA represent notable exceptions. These residues display enhanced insertion, likely driven by favorable hydrophobic interactions between their aligned side chains, in addition to interactions with lipid tails.

Although aurein and LLAA are sufficiently long to adopt well-defined amphipathic α-helical conformations, their lengths remain insufficient to span the lipid bilayer[11, 19, 20]. Consequently, peptide insertion is accompanied by characteristic tilt angles relative to the membrane plane. The tilt angle formed by the C-terminal to N-terminal vector ranges from 11°-17° for aurein and 23°-25° for LLAA. The larger tilt angles observed for LLAA are consistent with its greater insertion depth. This tilted insertion geometry is illustrated in Fig. 1.

To further characterize peptide-lipid interactions, radial distribution functions (RDFs) were computed using the GROMACS tool `gmx rdf`. The center of mass (COM) of each amino acid was selected as the reference point, while the COM of lipid phosphate groups served as target positions. The maximum RDF distance was set to 4 nm. Representative RDF profiles for a charged residue (Lys5) and a hydrophobic residue (Val9) in the 1LLAA-N-POPE/POPG (3:1) system are presented in Fig. 3.

The RDF analysis demonstrates that charged residues exhibit stronger correlations with negatively charged POPG phosphates compared with POPE phosphates. Furthermore, charged residues display higher RDF peaks relative to hydrophobic residues, indicating stronger interactions with lipid head groups. Collectively, these observations reinforce the dominant role of electrostatic interactions in governing peptide insertion, orientation, and selectivity. The enrichment of negatively charged lipids in bacterial membranes further explains the enhanced affinity and insertion behavior of these cationic peptides.

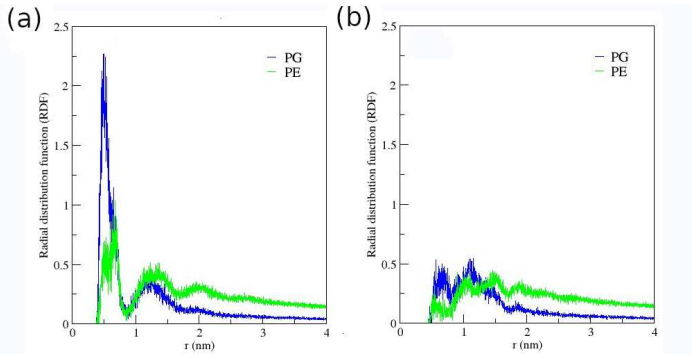


Fig. 3 Radial distribution functions (RDFs) between LLAA residues and lipid phosphates. The RDF was calculated between the center of mass (COM) of amino acids in LLAA and the phosphate groups of POPE (green line) and POPG (blue line) as a function of radial distance (nm). Reference residues are: (a) charged amino acid Lys5 and (b) neutral amino acid Val9.

These results indicate that both LLAA and aurein initially attach to the membrane surface via their N-terminal regions, followed by C-terminal insertion. LLAA exhibits stronger electrostatic interactions with negatively charged lipids in bacterial membranes, which facilitates deeper insertion relative to aurein and reflects its higher cationic charge. Residue-specific insertion patterns further suggest that electrostatic attraction between charged residues and phosphate head groups strongly influences peptide orientation and stability at the membrane interface. Overall, LLAA penetrates more extensively and forms stronger peptide-lipid interactions than aurein, consistent with its enhanced selectivity and activity toward bacterial membranes.

Five Vertical Peptides

To investigate the pore stability of aurein and LLAA, five peptides were initially arranged vertically in a pentagonal configuration inside DPPC and POPE/POPG (3:1) membranes. Fig. 4a shows an example of the initial pore structure. Simulations were carried out for 1 μs. Peptides are represented in helix form using the `cg-secondary-structure.tcl` and `la.tcl` scripts, while lipid tails are shown in line representation using `cg-bonds-v5.tcl`. Peptides are colored blue, red, green, purple, and yellow. Water molecules and lipid polar headgroup beads are shown in cyan and brown, respectively.

In the pre-formed aurein pore inside the POPE/POPG (3:1) bilayer without salt, the pore remained stable over 1 μs. Analysis of water molecules using a Tcl script showed that the number of waters quickly reached a constant value (Fig. 4c). Extending the simulation by 500 ns (total 1.5 μs) demonstrated that the pore remained open. In the presence of 0.15 M NaCl, the aurein pore persisted up to 1.3 μs (Fig. S**??**).

In contrast, in DPPC membranes, the five aurein peptides spontaneously aggregated. Water flow through the pore ceased, and the initial pore structure was disrupted at 700 ns in simulations with salt and 975 ns without salt. The peptides aggregated near the membrane surface (Fig. S**??**). Plots of water molecules inside these pores indicate that salt accelerates pore closure. Water counts were calculated based on the z-coordinates of the hydrophobic membrane region, with example plots for Pore-5aur-DPPC and Pore-5aur-DPPC-salt shown in Fig. S**??**.

Cheragi et al. [21] reported all-atom simulations of aurein and LLAA in DPPC bilayers, observing that 4 out of 5 aurein peptides formed stable pores with water flow until 1 μs. The differences with our coarse-grained results likely reflect accelerated dynamics inherent to coarse-grained models.

For LLAA, simulations in both DPPC and POPE/POPG (3:1) bilayers revealed rapid pore disassembly. Typically, one peptide remained vertically within the membrane while the others reoriented horizontally near the lipid headgroups. Addition of salt produced similar outcomes. Representative snapshots and water counts for Pore-5LLAA-POPE/POPG (3:1)-salt are shown in Fig. 4b, with other LLAA systems provided in Fig. S**??**.

Overall, these simulations highlight distinct behaviors of the two peptides. LLAA pores rapidly transformed into a single vertical peptide with four peptides lying horizontally at the lipidwater interface, consistent with the tendency of LLAA to act individually rather than cooperatively. In contrast, aurein pores remained stable longer, with

all five peptides maintaining vertical alignment for at least 750 ns. When aurein pores eventually collapsed, peptides aggregated near the headgroup region, similar to the clustering observed in five vertical peptide systems. This behavior aligns with experimental evidence of aurein's carpet-like and cooperative membrane-disrupting mechanisms [5, 9, 22].
Experimental studies report that aurein disrupts both eukaryotic and bacterial membranes once a critical surface concentration is reached, with thresholds dependent on membrane composition and phase [5, 23, 24]. Minor membrane disordering occurs at low concentrations, while higher concentrations can disrupt zwitterionic (eukaryotic) and anionic (bacterial) membranes. Consistent with these findings, our simulations show that aurein pores in POPE/POPG (3:1) bilayers are more stable than those in DPPC membranes.

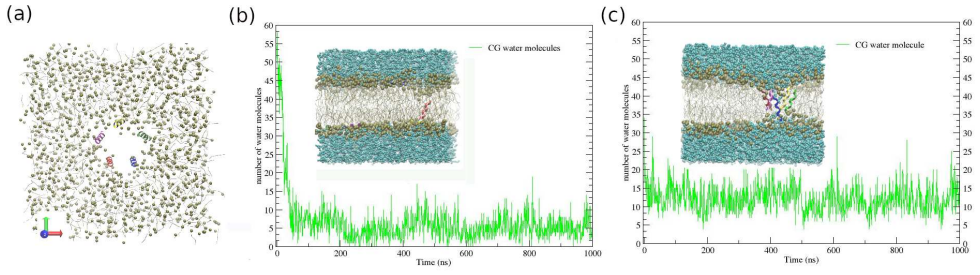


Fig. 4 Initial and final structure of aurein and LLAA peptides inside the POPE/POPG membrane, along with water molecule plots. (a) Initial pore structure at the membrane center. (b) LLAA pore reorganization and water content. (c) Aurein pore structure and water content over time.

The pore simulations emphasize distinct structural behaviors: aurein maintains stable vertical pores over hundreds of nanoseconds, suggesting cooperative alignment compatible with a transient barrel-stave-like mechanism. LLAA, however, rapidly disassembles, with most peptides reorienting parallel to the membrane surface, indicating a preference for surface adsorption and partial insertion. The observed stability differences, with aurein pores lasting longer in bacterial-like membranes and LLAA pores collapsing quickly, reflect the experimentally reported selective membrane activity of these peptides.

4 Conclusion

This study demonstrates that peptide concentration, peptide aggregation, and membrane composition strongly influence the interaction of aurein 1.2 and LLAA with lipid bilayers. LLAA displays stronger electrostatic interactions and deeper membrane insertion than aurein, whereas aurein exhibits greater cooperative behavior that promotes transient pore stabilization in bacterial membranes. These findings provide molecular-level insight into how subtle sequence differences govern antimicrobial peptide activity and remain consistent with recent experimental and computational studies.

5 appendix

For more details, see the Supplementary file.

References

[1] M.H.Khatami, M.Bromberek, I.Saika-Voivod, and V.Booth, "Molecular dynamics simulations of histidine-containing cod antimicrobial peptide paralogs in self-assembled bilayers," *Biochimica et Biophysica Acta (BBA) - Biomembranes*, 1838 (2014), 2778-2787.

[2] B.S.Perrin, R.Fu, M.L.Cotten, and R.W.Pastor, "Simulations of membrane-disrupting peptides II: AMP piscidin 1 favors surface defects over pores," *Biophysical Journal*, 111 (2016), 1258-1266.

[3] J.P.Ulmschneider, "Molecular simulation of antimicrobial peptides: mechanisms of membrane permeation and disruption," *Biochimica et Biophysica Acta (BBA) - Biomembranes*, 1838 (2014), 2266-2279.

[4] D.P.Tieleman, "Antimicrobial peptides in the cross hairs of computer simulations," *Biophysical Journal*, 113 (2017), 1-3.

[5] M.Shahmiri, M.Enciso, and A.Mechler, "Controls and constrains of the membrane disrupting action of aurein 1.2," *Scientific Reports*, 5 (2015), 16378.

[6] E.N.Lorenz?n, K.A.Riske, G.F.Troiano, G.C.A.Da Hora, T.A.Soares, and E.M.Cilli, "Effect of dimerization on the mechanism of action of aurein 1.2," *Biochimica et Biophysica Acta (BBA) - Biomembranes*, 1858 (2016), 1129-1138.

[7] T.Rozek, K.Wegener, J.H.Bowie, I.N.Olver, J.A.Carver, J.C.Wallace, and M.J.Tyler, "The antibiotic and anticancer active aurein peptides from the Australian bell frogs Litoria aurea and Litoria raniformis," *The FEBS Journal*, 267 (2000), 5330-5341.

[8] X.Li, Y.Li, A.Peterkofsky, and G.Wang, "NMR studies of aurein 1.2 analogs," *Biochimica et Biophysica Acta (BBA) - Biomembranes*, 1758 (2006), 1203-1214.

[9] D.I.Fernandez, A.P.Le Brun, T.C.Whitwell, M.Sani, M.James, and F.Separovic, "The antimicrobial peptide aurein 1.2 disrupts model membranes via the carpet mechanism," *Physical Chemistry Chemical Physics*, 14 (2012), 15739-15751.

[10] D.I.Fernandez, M.Sani, A.J.Miles, B.A.Wallace, and F.Separovic, "Membrane defects enhance the interaction of antimicrobial peptides, aurein 1.2 versus caerin 1.1," *Biochimica et Biophysica Acta (BBA) - Biomembranes*, 1828 (2013), 1863-1872.

[11] E.E.Ambroggio, F.Separovic, J.H.Bowie, G.D.Fidelio, and L.A.Bagatolli, "Direct visualization of membrane leakage induced by the antibiotic peptides: Maculatin, Citropin, and Aurein," *Biophysical Journal*, 89 (2005), 1874-1881.

[12] D.K.Rai and S.Qian, "Interaction of the antimicrobial peptide aurein 1.2 and charged lipid bilayer," *Scientific Reports*, 7 (2017), 3719.

[13] D.Van Der Spoel, E.Lindahl, B.Hess, G.Groenhof, A.E.Mark, and H.J.C.Berendsen, "GROMACS: Fast, flexible, and free," *Journal of Computational Chemistry*, 26 (2005), 1701-1718.

[14] G.Wang, Y.Li, and X.Li, "Correlation of three-dimensional structures with the antibacterial activity of a group of peptides designed based on a nontoxic bacterial membrane anchor," *Journal of Biological Chemistry*, 280 (2005), 5803-5811.

[15] M.S.Balla, J.H.Bowie, and F.Separovic, "Solid-state NMR study of antimicrobial peptides from Australian frogs in phospholipid membranes," *European Biophysics Journal*, 33 (2004), 109-116.

[16] G.Bussi, D.Donadio, and M.Parrinello, "Canonical sampling through velocity rescaling," *The Journal of Chemical Physics*, 126 (2007), 014101.

[17] H.J.C.Berendsen, J.P.M.Postma, W.F.van Gunsteren, A.DiNola, and J.R.Haak, "Molecular dynamics with coupling to an external bath," *The Journal of Chemical Physics*, 81 (1984), 3684-3690.

[18] W.Humphrey, A.Dalke, and K.Schulten, "VMD: Visual molecular dynamics," *Journal of Molecular Graphics*, 14 (1996), 33-38.

[19] A.A.Bahar and D.Ren, "Antimicrobial peptides," *Pharmaceuticals*, 6 (2013), 1543-1575.

[20] G.E.Balatti, E.E.Ambroggio, G.D.Fidelio, M.F.Martini, and M.Pickholz, "Differential interaction of antimicrobial peptides with lipid structures studied by coarse-grained molecular dynamics simulations," *Molecules*, 22 (2017), 1775.

[21] N.Cheraghi, M.Hosseini, and S.Mohammadinejad, "Pore formation and the key factors in antibacterial activity of aurein 1.2 and LLAA inside lipid bilayers: a molecular dynamics study," *Biochimica et Biophysica Acta (BBA) - Biomembranes*, 1860 (2018), 347-356.

[22] M.A. Sani, E. Gagne, J.D. Gehman, T.C. Whitwell, and F. Separovic, "Dye-release assay for investigation of antimicrobial peptide activity in a competitive lipid environment," *European Biophysics Journal*, 43 (2014), 445-450.

[23] S. Praporski, A. Mechler, F. Separovic, and L.L. Martin, "Subtle differences in initial membrane interactions underpin the selectivity of small antimicrobial

peptides," *ChemPlusChem*, 80 (2015), 91-96.

[24] A. Mechler, S. Praporski, K. Atmuri, M. Boland, F. Separovic, and L.L. Martin, "Specific and selective peptide-membrane interactions revealed using quartz crystal microbalance," *Biophysical Journal*, 93 (2007), 3907-3916.

[25] C. Wang, Y.-H. Ma, X. Han, and X. Lu, "Re-Examining Interaction between Antimicrobial Peptide Aurein?1.2 and Model Cell Membranes via SFG," *Langmuir*, 39 (2023), 690-699.

[26] E. A. Ermakova and R. Kh. Kurbanov, "Interaction of Uperin Peptides with Model Membranes: Molecular Dynamics Study," *Membranes*, 13 (2023), 370.

[27] Males, Matko and Zoranic, Larisa, "Simulation Study of the Effect of Antimicrobial Peptide Associations on the Mechanism of Action with Bacterial and Eukaryotic Membranes," *Membranes*, 12 (2022), 891.

Acknowledgements

The author gratefully acknowledges Dr. Sarah Mohammadinejad for conceiving the study, providing computational resources at IASBS, and for her guidance and valuable discussions throughout this work. The author also thanks Dr. Leila Hassani for valuable discussions and support.

Funding Declaration

The authors declare that no funding was received for this work.

Supplementary Files

This is a list of supplementary files associated with this preprint. Click to download.

- RAnsarihaghiMSCsupplementary.pdf